

## Modelling the impact of Urban Heat Island mitigation strategies on Urban Air Quality

NEHA M. DAVE<sup>1\*</sup>, RUPESH P. VASANI<sup>2</sup> and PARMIT CHHASIYA<sup>3</sup>

<sup>1</sup>Environment Engineering, Gujarat Technological University, Ahmedabad, India.

<sup>2</sup>Sal Institute of Technology & Engineering Research, Ahmedabad, India.

<sup>3</sup>Center for Applied Geomatics, Cept Research and Development Foundation, Cept University, Ahmedabad, India.

### Abstract

Increasing urban sprawl has caused many severe problems like surge in pollution, rapid climatical variations, and the intensification of temperature in the urban areas, termed Urban Heat Islands (UHI). Population density has caused the conversion of most land areas into cities, and cities have expanded vastly. UHI phenomenon has caused temperature rise in the cities. Most of the metropolitan regions of India are experiencing consequences of UHI and the severity of pollution formation, which is a crucial research area. Since the rising temperature has a direct linkage with urban air pollution, the mitigation measures for UHI are also linked with urban air pollution mitigation, efficacy of mitigation measures of UHI phenomenon in correlation with urban air quality is being studied extensively, which emphasizes the scientific approach and planning concerns of implementation agency to consider the same into urban design and planning aspects. Ahmedabad is one of the growing metropolitan regions of India. The city has grown economically and physically by expanding its boundaries in a radial pattern. This study has attempted temporal assessment of remote sensing data to derive the UHI and the city's growth, and its changing land uses. Assessment has been performed from 2008 to 2018 from Landsat data for temperature profile at surface level and type of usage of land of the study area. The spatial profile of Particulate Matter (PM<sub>2.5</sub> and PM<sub>10</sub>) has been generated based on data from the state pollution control board. Four variables, LST, PM<sub>2.5</sub>, PM<sub>10</sub>, and LULC, are taken to establish the relationship between all variables present in different layers with the help of regression statistical analysis. A strong positive correlation between PM<sub>2.5</sub>, PM<sub>10</sub>, and LST has been discovered, which was eventually used to assess the impact of mitigation strategies of UHI, specifically urban greening and a white roof to particulate matter concentrations.



### Article History

Received: 10 March 2021

Accepted: 17 June 2022


### Keywords

Ahmedabad City;  
Air Quality;  
Regression Analysis;  
Urbanization;  
Urban Heat Island.

**CONTACT** Neha M. Dave ✉ nmd\_env@yahoo.com 📍 Environment Engineering, Gujarat Technological University, Ahmedabad, India.



© 2022 The Author(s). Published by Enviro Research Publishers.

This is an  Open Access article licensed under a Creative Commons license: Attribution 4.0 International (CC-BY).

Doi: <http://dx.doi.org/10.12944/CWE.17.2.11>

## Introduction

Urban Heat Islands is the higher temperature in an urban area than in surrounding open or rural areas which has two distinct categories: Atmospheric and Surface Heat Island. Atmospheric UHIs are divided into two parts. one is the layer of air to the top of trees or roofs, and another is from the building roof or tree top level to the upper atmosphere of that area. Surface urban heat island depicts a difference between urban surfaces compared with its surrounding. The surface UHI is highest during the summer, and its variation is much more than UHIs.<sup>11</sup> The spatial characteristics of the UHI are related to the topography profile of the urban area, which can be differentiated by the urban-rural temperature boundary.<sup>10</sup> Moreover, urban area expands at a rapid rate from center to fringes. The growth generally happens in areas of city fringes, thus exacerbating the sprawling level. Changing scenarios of human settlements, lifestyle changes, and anthropogenic activities have resulted in two major phenomena, increasing heat and deterioration of air quality.

Urban Heat Islands cause higher use of energy for cooling.<sup>1</sup> Heat also produces chemical reactions into atmosphere.<sup>2</sup> These secondary air pollutants harm health of living beings.<sup>3</sup> Urban green areas and white roofs decrease heat in atmosphere and eventually improves air quality.<sup>4</sup>

Urban Heat Island intensity, also known as UHI magnitude, is the temperature difference between urban and surrounding areas.<sup>5</sup> Climate region, local topography, and industry expansion of a city affect UHI intensity.<sup>6</sup> LULC characteristics, the neighborhood rural areas,<sup>7</sup> and quantity of vegetation in an urban area<sup>8</sup> are remarkable for urban heat island intensity, as well as local climatic thermal patterns. It is evaluated that 3-8% higher electricity demand in an urban area with a population of more than 1 00,000 is used to tackle the heat enhanced by the urban heat island effect, which leads to higher emissions enhancing the concentration of harmful smog, higher air pollution, and human health impacts.

Through state-of-the-art satellite technology, land surface temperature has become a key parameter for estimating surface temperature.<sup>9</sup> Satellite sensor, having a thermal band, targets towards surface

and radiance value which is further converted into ground-level reflectance value.

UHI mitigation measures such as green area development and change of materials which are able to reduce the adverse effects of the UHI and mitigate future problems.<sup>14</sup> Considering variables of the urban atmosphere such as evaporation, humidity, temperature, turbulences, etc., UHI mitigation strategies result in energy consumption and changes in radiation patterns.<sup>15</sup>

## Literature Studies

Anthropogenic activity affects the urban climate, and its effects are adverse to the environment. Change in the local natural environment, which is replaced by artificial with concrete and other radiation absorption materials, affects the urban area's heat exchange and micro climate. Urbanization changes the LULC characteristics of an area, resulting in the formation of the UHI effect. Built-up area increase, vegetation decrease, emission, and pollution are reasons for urban areas hotter than green fields. Urban climate study in South Asia shows more than an 8 °C temperature difference between the highly-dense urban area and greenfields.<sup>8</sup> Even high-temperature rises in urban areas end up with high energy consumption, which comes from the area covered by buildings and streets as an impermeable material with low emissivity and high heat absorption.

Remote sensing can map urban areas and their LULC spatial concentration using several classification methods as captured optical data with spectral information about the area. Land Surface Temperature (LST) is a necessary term related to the thermal state of the boundary layer of the study area. Initially, the land surface temperature was coined for surface or air temperature measured by a thermometer installed 1.5-3.5 meters above the flat surface. Due to advancements in satellite technology, another type of land surface temperature data collection, satellite-based surface temperature collection, i.e., skin temperature, is extremely useful when the spatial scale is large.<sup>10</sup> Through state of the art satellite technology, land surface temperature has become a key parameter to estimate surface temperature, which is not the only affecting indicator of climate change but also its

relation with radiation, nevertheless with control of surface sensibility and heat flux exchange between atmosphere and surface of the earth.<sup>5</sup> For instance, energy exchange in boundary UHI is dominated by the disparity between air temperature and surface temperature. The air and the surface interact with different time-space scales to external forces, yet they are correlated complexly.

The satellite sensor, having a thermal band, targets the surface, and the radiance value is further converted into a ground-level reflectance value. The reflectance from the ground is converted to the top of the atmosphere radiance value. The Thermal Infrared Sensor (TIR) gets the surface radiance radiated towards the sensor until this value is converted to brightness temperature. To derive Land Surface Temperature, it is must require to calculate surface emissivity (E).

Urban heat island contributes to elevated ozone levels because it adds thermal radiation to a chemical reaction from the ground ozone level. Sunlight and enhanced heat levels due to the urban heat island effect can also photochemically cook ozone to a more hazardous level when air temperature exceeds 90°C; ozone is created when dinitrogen monoxide and volatile organic compounds photochemically combine with solar radiation. Nevertheless, the ozone concentration can be reduced by the lower ambient air temperature. Under the right chemical conditions, the UHI effect can hike up the air temperature by 10 F or more. thus, it acts an additive supportive effect to solar radiation.

Climate region, local topography, and industry expansion of a city affect UHI intensity,<sup>12</sup> green roofs have capacity of surface cooling which is very significant and can help in decreasing temperature in urban areas,<sup>16</sup> LULC characteristics, the neighborhood rural areas,<sup>3</sup> and quantity of vegetation in urban area<sup>2</sup> are remarkable for urban heat island intensity, as well as local climatic thermal patterns. It is evaluated that 3-8% higher electricity demand in urban areas with a population of more than 1,00,000 is used to tackle the heat enhanced by the urban heat island effect, which leads to higher emission of SO<sub>2</sub>, CO, NO, PM2.5, PM10, enhancing the concentration

of harmful smog, higher air pollution, and human health impacts.

PM2.5 shows a positive correlation with change of usage pattern of land with a correlational coefficient of more than 0.6. The area with more road density, sizeable built-up area, and LST are steady with a high focus on PM and SO<sub>2</sub>, NO<sub>2</sub> and CO, which can be understood by the correlation between air pollutants and land use.<sup>9</sup> Furthermore, NO<sub>2</sub> is the most sensitive gas affected by land-use changes, and O<sub>3</sub> shows a weak correlation with land use. The relational study between UHI and air quality shows that increasing UHI increases particulate matter. Decrease in Ozone concentration is observed with usage of high albedo built up.<sup>14</sup> Moreover, vegetation of the urban area and high emissivity rooftops could drastically reduce energy consumption, resulting in improved air quality.<sup>4</sup>

The arrangement of UHI is, for the most part, supported by the low wind speed and high convergence of PM2.5, with a positive relationship between the UHI and PM2.5 focuses. The expanded pressurized canned products in urban climates lessen the approaching solar flux and increment of barometrical long wave radiation in the urban areas. The reaction of the material to the difference in reflected radiation is solid during the evening and powerless during the day. The surface urban heat island force is improved by 12% in the evening by the expanded assimilated solarradiation in the urban areas.

### Methodology

This study is limited to the boundary of Ahmedabad Municipal Corporation. Ahmedabad was declared a Megacity, located between a latitude of 23.03 and a longitude is 72.58 in North-central Gujarat. The average elevation profile of Ahmedabad city is 53 meters. The population of Ahmedabad is more than 3.5 million as per the census 2001, which is the 7<sup>th</sup> metropolitan city of India. Ahmedabad is located on the Sabarmati River.

Ahmedabad has a dry and comparatively hot climate with maximum 41°C and minimum 27°C in summer months and maximum 30°C and minimum 15°C in winter months with average rainfall of 800 mm.

In order to begin this study, primary data was collected from various sources. Collected data was in a standard format, so it was needed to select, acquire, review and process it for further analysis relevant to the study. Raster Data in terms of Satellite Images were acquired from Landsat TM & ETM+ Data (2008 to 2018). Vector Data such as study area boundary, ward, zones of the city, physical features like rivers and lakes, green areas, etc. were prepared based on secondary data sources of Ahmedabad Municipal corporation, Attribute Data of Air Quality for PM<sub>2.5</sub> and PM<sub>10</sub> (2008, 2015-2017) were acquired from State Pollution Control Board.

The identified data types can be categorized into Raster, Vector, and Non-Spatial (Attribute Data). Raster Data Landsat TM & ETM+ data is used for LST generation and LULC classification of the study area. Vector data like administrative boundaries of the study area helps perform numerous geospatial operations that bounds research to the study area. In Non-Spatial or Attribute data, data of Air Quality focused on PM<sub>2.5</sub> and PM<sub>10</sub> of Ahmedabad city has been collected from GPCB. Moreover, Field data collection, which is done by ground-truthing, gives ground-based LST and Air Quality data. The flow chart shows various spatial processes for study, such as the LST retrieval process, supervised classification for LULC, Spatial interpolation for Air Quality data, etc.

Furthermore, a study has been divided into the scale of study. Macro level, Meso level, and Micro level, which leads to spatial modeling of LST, Air Quality, and LULC. The study is progressed by suggestive mitigation measures for UHI and Air Quality for the study area. Further geospatial operations and methods are explained below, used for this study. Ground truthing has been done for LST results and analysis of the data gap between in-situ measurements. Ground truthing dates are selected based upon satellite temporal resolution of Landsat-8, moreover, the study area for ground-truthing has been done based upon the typology of area, for readings types of features are identified for temperature measurement.

Moreover, Field data collection, which is done by ground-truthing, gives ground-based LST and Air Quality data. The flow chart shows various spatial processes for study, such as the LST retrieval

process, supervised classification for LULC, Spatial interpolation for Air Quality data, etc. Furthermore, the study has been divided into scales: Macro level, Meso level, and Micro level, which leads to spatial modelling of LST, Air Quality, and LULC. The study is progressed by suggestive mitigation measures for UHI and Air Quality for the study area. Further geospatial operations and methods are explained below for this study. Ground truthing has been done for LST results and analysis of the data gap between in-situ measurements. Ground truthing dates are selected based upon the satellite temporal resolution of Landsat-8. Moreover, the study area selection for ground-truthing has been made based on the typology of the area, for readings, types of features are identified for temperature measurement.

Model Builder in Arc GIS is used for processing the databases. It is an application that automates geoprocessing workflows, a series of tools chained together, where the output of one tool is given as input to another tool. After having connected tools in the Model, one can execute and run that model. In simple words, it connects geoprocessing sequences and gives desired spatial output. In the case of LST derivation, it saves time if there is a model system that contains sequences of raster equations. Hence, a model was created to estimate LST, containing its intermediate products, e.g., Radiance, Emissivity, and Fractional vegetation cover. Image classification for land use/land cover is the process of developing interpreted maps from remotely sensed images. Consequently, classification gives the most important visualization and spatial information for usage pattern of land. To derive spatial relation of land use/land cover with LST, Air Quality, it is needed to process image classification through satellite imagery for the Ahmedabad region. The Landsat images (2008 to 2018) are classified to get the land cover patterns in Ahmedabad. The classes are identified from a range of pixel values, tone variance, visual image interpretation of the image, and histogram peaks. Identified classes for this study are Built-up, Open Land, Vegetation, and Waterbody.

The three-dimensional interpolation method is used to estimate the value of unknown points by known points, and it is used to predict unknown values by existing spatial values. For instance, we have a data variable that has a spatial value at each point

(e.g., elevation, temperature, etc.), but the data variable is not spatially distributed; hence it is required to produce a continuous raster surface that can give the predicted value of other points based upon existing points.

Air Quality, PM2.5, and PM10 data collected from GPCB are attribute data brought in point shape files. Based on available points, it was needed to generate a surface for the AMC study area so that Air Quality (PM2.5 and PM10) can also be predicted where a collection point is not available.

Inverse Distance Weighting is finally used to connect all raster and vector database. Ground truthing for temperature and air quality of the study area has been done for two zones, the Central and West zone of Ahmedabad. The date selection is made according to the satellite temporal resolution, for Landsat-8, it is

16 days. The central and West zone is selected for Ground truthing because of building typology, land cover feature, and built-up density. Measurement of temperature for features like the wall, open land, road, vegetation, and waterbody has been taken by IR Gun and PM2.5 and PM10 by Polludrone sensor. Regression analysis is used here for derivation of co relation of two or more two variables.

**Data Analysis and Interpretation**

Trend Analysis of LST, Air Quality, and LULC was done to get series information with respect to time. It is a statistical technique that deals with data with respect to intervals; this interval is a time. In the case of LST, two seasons, summer and winter of the year 2008 to 2018, in which 2008, 2015 from 2018 are chosen for trend analysis. The calculated LST are divided into ranges for both summer and winter seasons to preserve symbology for visualization.

**Table 1: Values of Lst In °C for Summer and Winter Seasons**

Study year	Average °C	Highest °C	Lowest °C	Study year	Average °C	Highest °C	Lowest °C
2008	40.26	53.85	26.68	2008	25.30	30.43	20.18
2015	30.60	36.98	24.23	2015	21.05	26.78	15.32
2016	35.35	43.95	26.65	2016	24.33	29.66	18.94
2017	41.95	54.41	29.39	2017	25.89	31.24	20.54
2018	35.77	44.16	27.39	2018	22.95	28.06	17.85
For Summer				For Winter			

Statistics show that there has been a temperature rise in the summer and winter seasons in the year 2017. The mean temperatures for both the summer and winter seasons of 2008-2018 are 36°C and 23°C, respectively.

For Summer in 2008 temperature recorded was 40.26 °C; it increased to 41.95°C in 2017, and 35.77°C temperature was recorded in 2018. The maps below show temporal changes in LST for the Summer season.

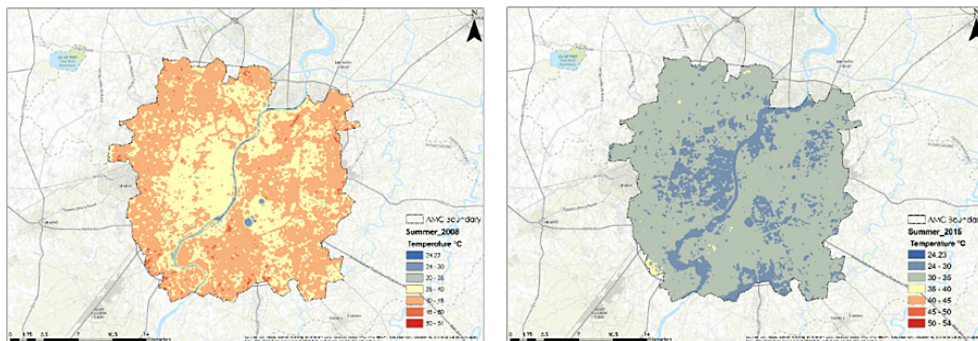


**Fig. 1**



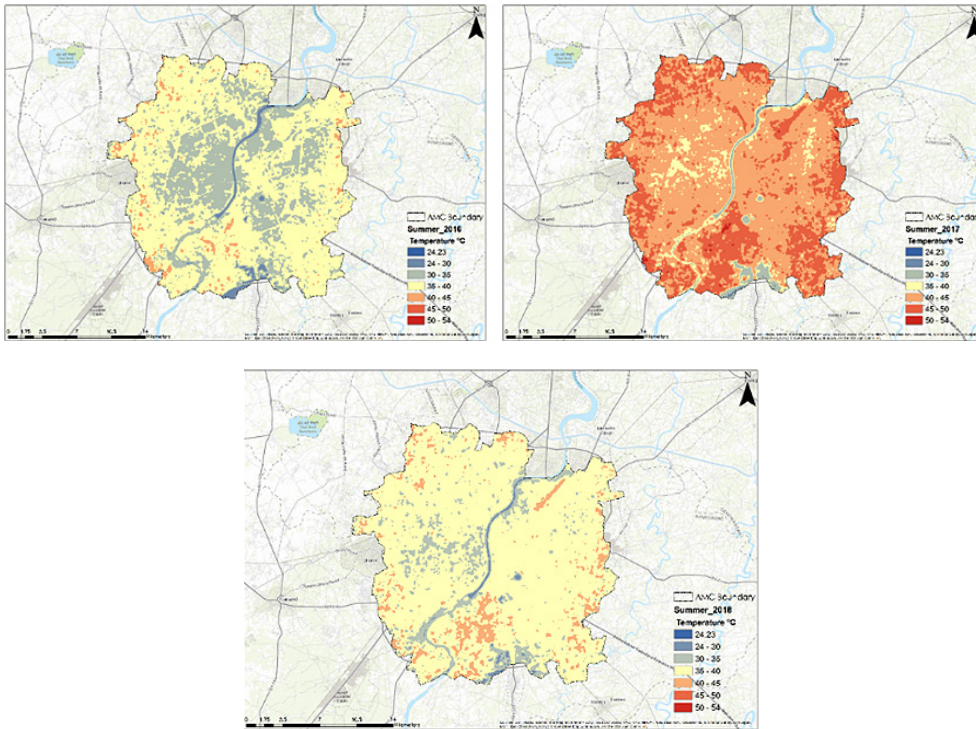
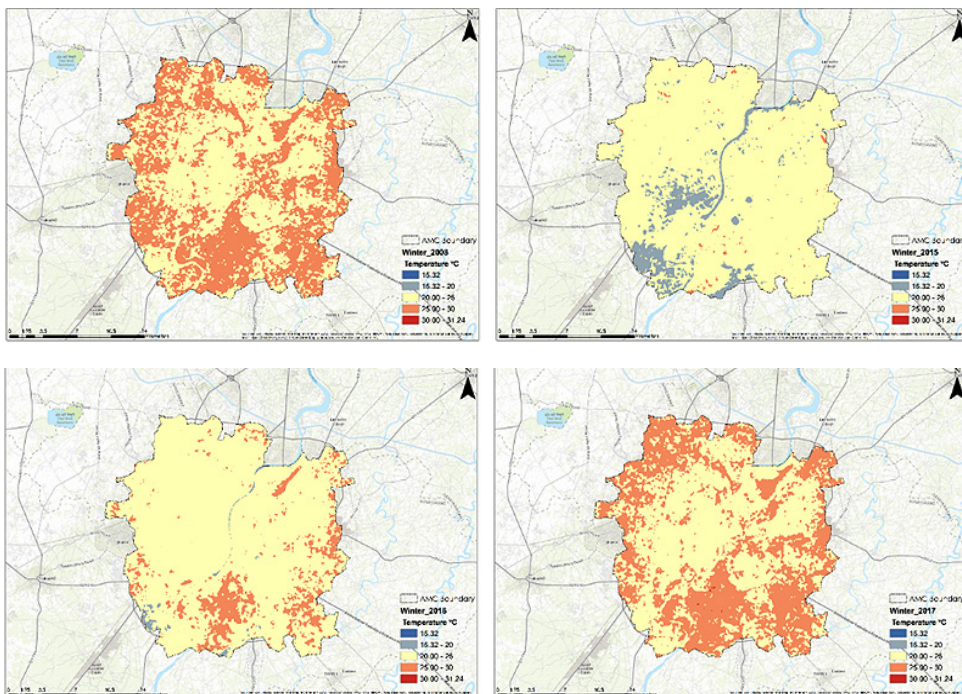


Fig. 2

For Winter, In 2008 temperature recorded was 25.30°C; it increased to 25.89°C in 2017, and 22.95°C temperature was recorded in 2018.

The maps below show temporal changes in LST for the Winter season.



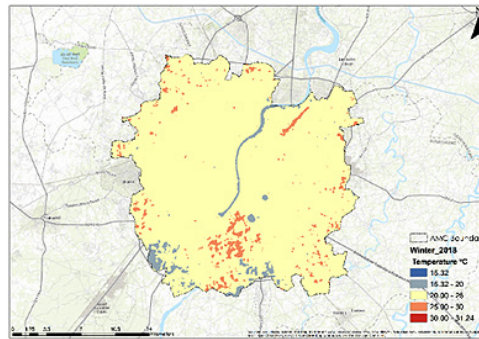


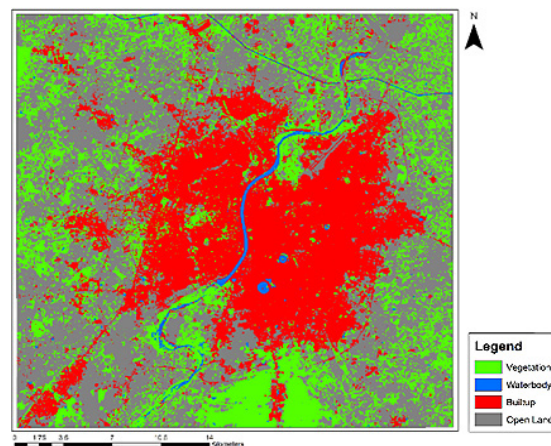
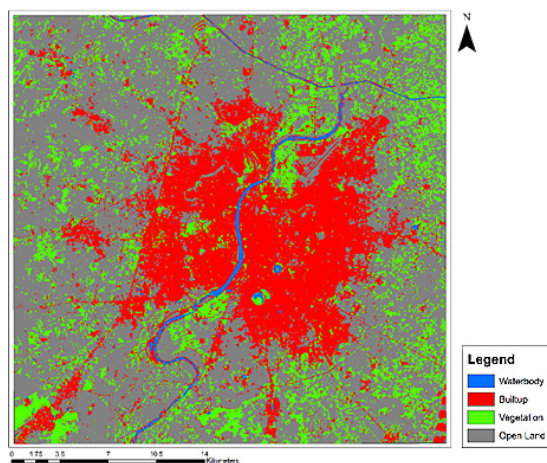
Fig. 3

Landcover classes that impact UHI are Built-up, Non-Built-up, Vegetation, and Waterbody. Through the supervised classification, method results are carried out in raster. The classes are identified from the range of pixel values, the variance of the tone, visual image interpretation of the image,

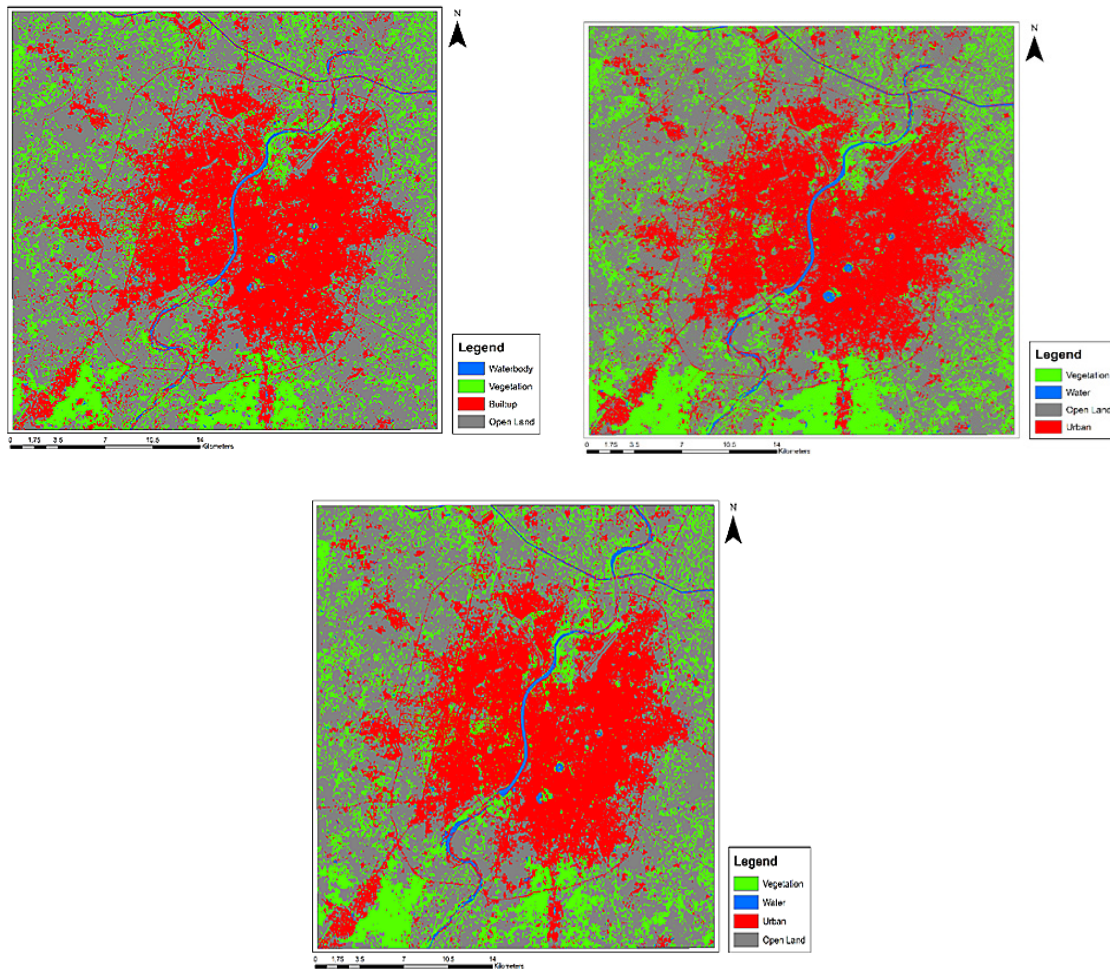
and histogram peaks. Identified classes for this study are Built-up, Open Land, Vegetation, and Waterbody. The table below shows the total landcover change identified through the generated raster from the supervised classification method.

Table 2: Land Cover Class Area (In Sq.Km)

Landcover class	2008	2015	2016	2017	2018
Urban	163.97	240.19	243.10	248.76	253.96
Vegetation	134.64	120.66	118.55	117.54	116.35
Waterbody	6.71	7.25	8.65	9.65	10.58
Open land	112.13	84.92	82.67	79.65	78.65







**Fig. 4: The proportion of built up areas was estimated across the Ahmedabad Municipal corporation area.**

Statistics show that open land has the highest noted temperature value than other classes, moreover, waterbody has the least temperature compared to other land cover class. From 2008 to 2018, it can be observed that trend of temperature rise has increased with time. It can be observed from the below table that, for the Winter season, the average temperature of vegetation class was 20.28 °C in 2008, while it increased in 2018 up to 21.83°C. The average temperature of Waterbody was 18.65 °C in 2008 while it increased in 2018 up to 20.31°C, the average temperature of the Urban class was 21.01 °C in 2008 while it increased in 2018 up to 22.32°C, and the average temperature of open land was 22.65 °C in 2008 while it increased in 2018 up to 22.85°C. For the Summer season, the average temperature of vegetation class was 31.26 °C

in 2008 while it increased in 2018 up to 34.58°C, the average temperature of Waterbody was 28.63 °C in 2008 while it increased in 2018 up to 31.27°C, the average temperature of the Urban class was 40.21 °C in 2008 while it increased in 2018 up to 41.95°C, the average temperature of open land was 39.78 °C in 2008 while it increased in 2018 up to 42.13°C.

Raster surface for attribute data of Air Quality (PM2.5 and PM10) of Ahmedabad city is derived through interpolating variables. For winter and Summer, a raster surface for PM2.5 and PM 10 is generated for both seasons. Data of PM10 was available for winter and summer from 2008 to 2017, while data of PM2.5 was not available for study for 2008; from 2015 to 2017, data of PM2.5 was taken for study.



**Table 3: Values Of Lst In °C Per Land Cover Classes**

	2008	2015	2016	2017	2018		2008	2015	2016	2017	2018
Vegetation	20.28	21.23	22.27	24.62	21.83	Vegetation	31.26	29.75	33.86	38.95	34.58
Waterbody	18.65	19.82	21.06	22.97	20.31	Waterbody	28.63	27.55	30.4	35.85	31.27
Urban	21.01	21.67	22.83	24.59	22.32	Urban	40.21	30.98	35.62	42.73	41.95
Open land	22.65	22.09	23.32	25.31	22.85	Open land	39.78	32.25	37.67	44.71	42.13
Average LST in Landcover Classes for Winter						Average LST in Landcover Classes for Summer					

**Table 4: Pm2.5 and Pm10 Statistics for Winter and Summer Seasons**

Study Year	PM10 concentration (µg/m3)	PM2.5 concentration (µg/m3)	Study Year	PM10 concentration (µg/m3)	PM2.5 concentration (µg/m3)
2008	108.52	N.A.	2008	102.75	N.A.
2015	84.04	30.50	2015	96.41	37.74
2016	110.41	51.44	2016	102.27	30.45
2017	125.31	64.29	2017	116.15	41.53
For Winter			For Summer		

From the above table, it can be observed that, for the winter season, PM10 in 2008 was 108.52 µg/m<sup>3</sup> and raised in 2017 upto 125.31µg/m<sup>3</sup>, PM2.5 in 2015 was found to 30.50 µg/m<sup>3</sup> and increased 64.29 µg/m<sup>3</sup>.

For the Summer season, PM10 in 2008 was 102.75 µg/m<sup>3</sup> and raised in 2017 upto 116.15µg/m<sup>3</sup>; PM2.5 in 2015 was found at 37.74 µg/m<sup>3</sup> and increased to 41.53 µg/m<sup>3</sup>. It is noticeable that the trend of PM10 and PM2.5 from 2008 to 2017 is increasing.

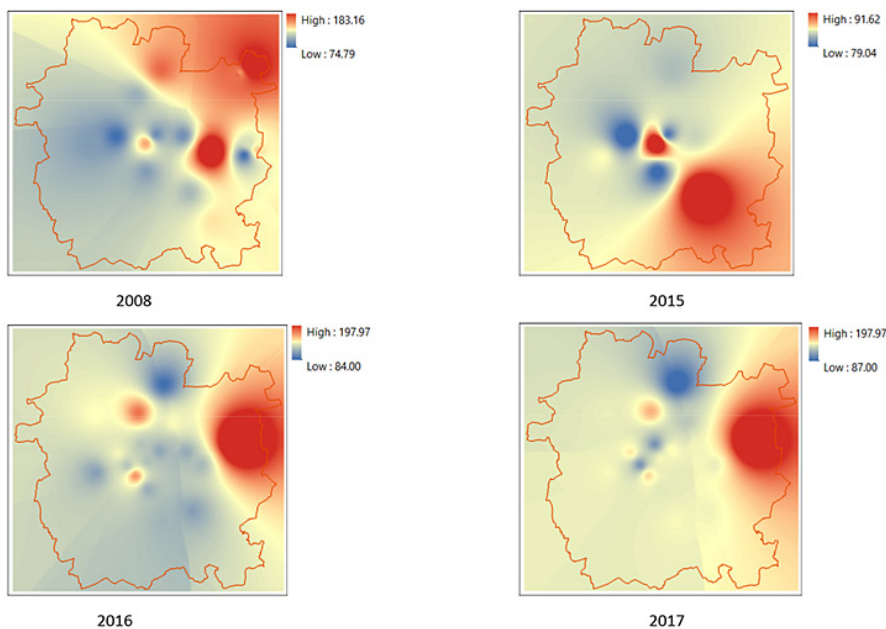


**Fig. 5: Interpolated maps of PM10 for Winter season (values are in µg/m<sup>3</sup>)**

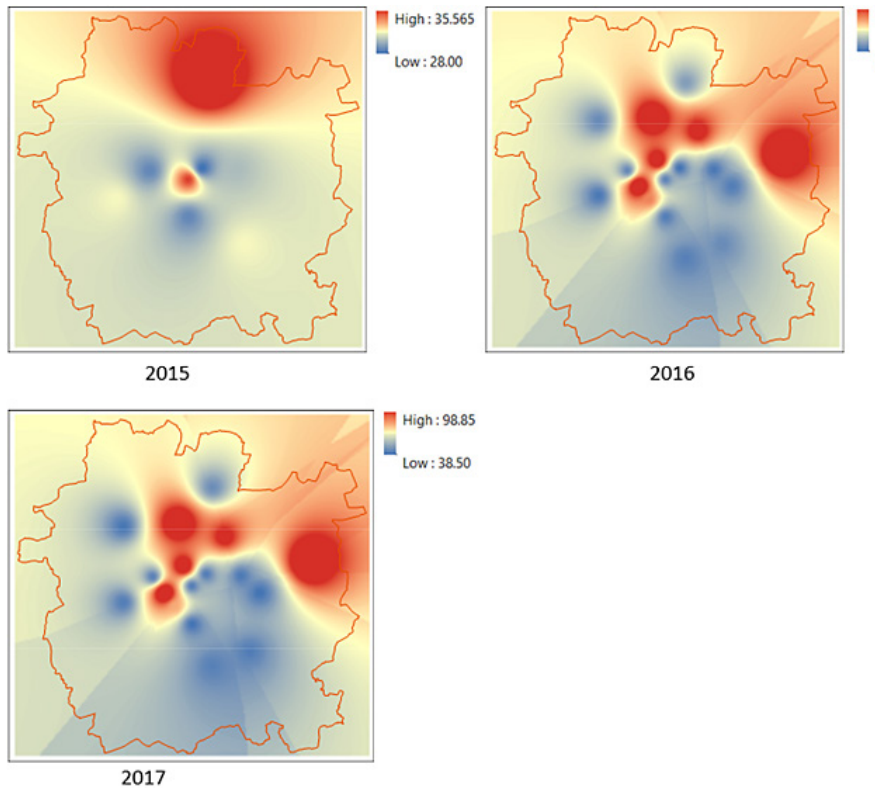


**Fig. 6: Interpolated maps of PM<sub>2.5</sub> for Winter season (values are in  $\mu\text{g}/\text{m}^3$ )**

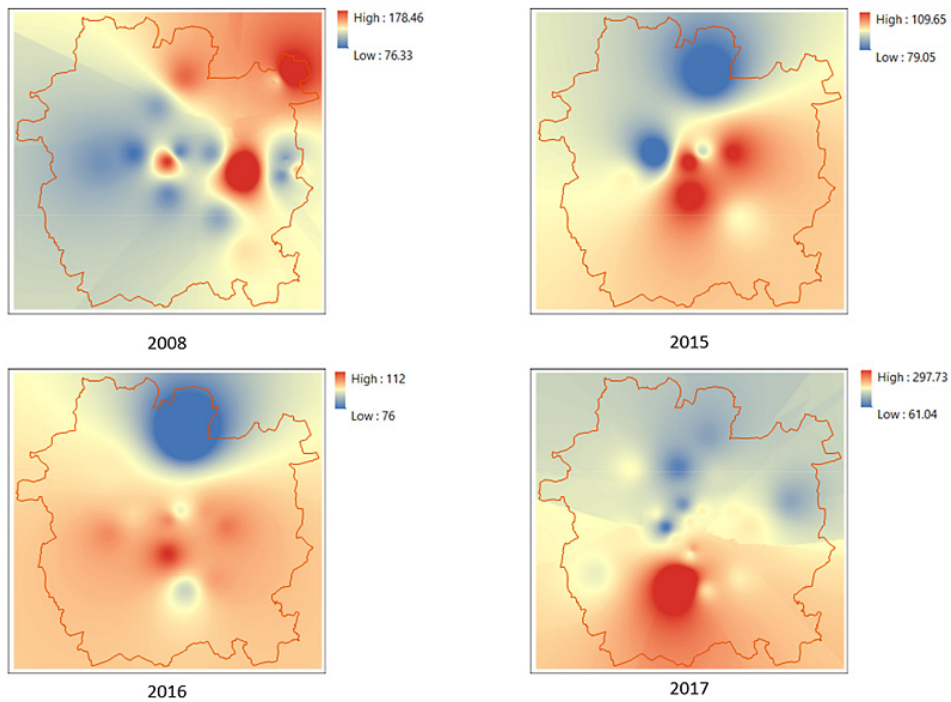


**Fig. 7: Interpolated maps of PM<sub>10</sub> for Summer season (values are in  $\mu\text{g}/\text{m}^3$ )**

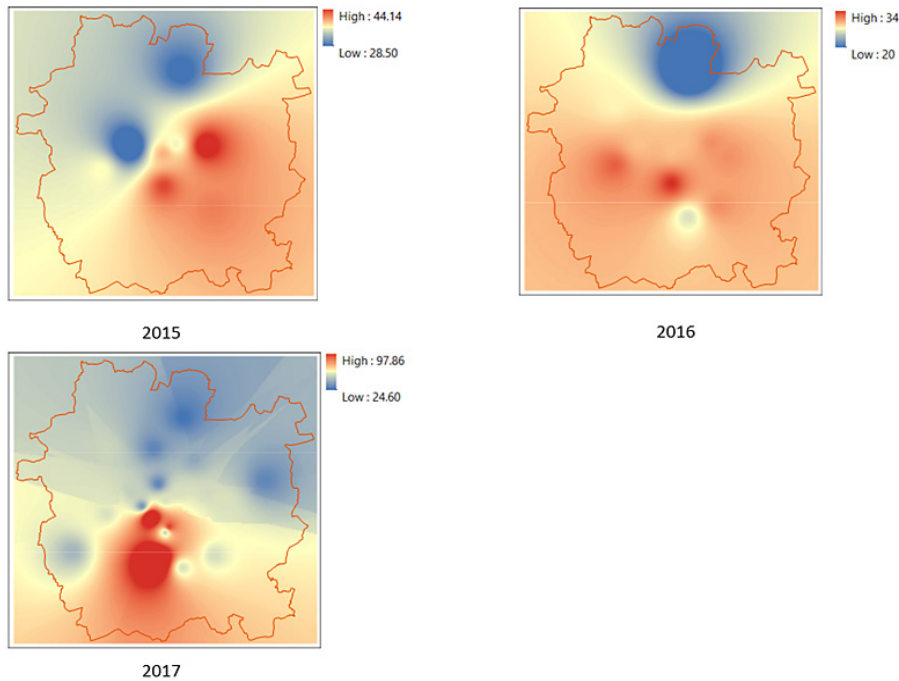


**Fig. 8: Interpolated maps of PM2.5 for Summer season (values are in µg/m3)**

To generate fishnet for the AMC region, spatial extent is considered per AMC boundary, and grid size is taken 120\*120m. Landsat spatial resolution is 30m; thus, to get the overall average scenario of LST, Air Quality, and LULC in grid level, the smallest grid size containing 16 pixels is 120\*120m. The total number of cells generated is 47,073.

cell values of LST, LULC, and Air Quality (PM2.5 and PM10) is to analyze the relationship of these layers within each cell. All values falling under the AMC region have been transferred using Zonal statistics to grids of 120\*120m. The attribute table of the grid after using zonal statistics is shown below. Total rows in grid's attribute table are 47,073.

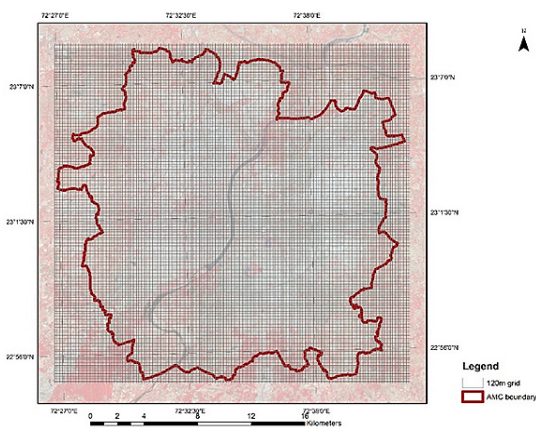


**Fig. 9**

Zonal statistics is a tool that estimates cell statistics or a value of a raster layer by a defined zone. To transfer the value of LST, LULC, and Air Quality (PM2.5 and PM10). The idea of transferring

The simple linear regression model uses the following equation with independent and dependant values.

$$Y = a + bX + \epsilon$$

Where: y – dependent variable, x – independent variable, a – intercept, b – slope,  $\epsilon$  – residual/error

In this study, there are four variables, LST, PM2.5, PM10, and LULC. In order to perform regression analysis, the Multilinear regression method has been used. To predict LST, it is taken as a dependent variable, while LULC classes are taken as independent variables.

Regression Statistics derived were Multiple correlation coefficient 0.809074773, Coefficient of determination 0.654601988, Adjusted



Coefficient of determination 0.654558728, Standard Error 9.022893242 for Observations 40773.

The value of  $R^2$  is 0.65, which is a positive correlation, which means the independent variable explains 65.45% of the variance in the dependent variable.

The multiple linear regression is expressed here as,  $LST = 32.86 + 0.09 * UrbanP + 0.13 * OpenP + 0.038 * VegP$

Where, LST= Land Surface Temperature, 32.86= Intercept, UrbanP= Percentage of Urban, OpenP= Percentage of Open land, VegP= Percentage of Vegetation

In the equation, it was observed that WaterP (Percentage of Water), coefficient value coming null, the fact that only 10% of the total land-use area of AMC having Landcover class of Waterbody. It was attempted to select only grids with waterbody as landcover class. Thus, grids with a water area percentage of more than 50% were selected through a query, and 679 grids were selected. For these 679 grids, multilinear regression was computed, and the value of  $R^2$  computed at 0.314, which is a negative correlation.

Furthermore, it was expanded to a multi-linear regression equation derived before, which has no significance due to data insufficiency of waterbody class. Regression Statistics derived were, Multiple correlation coefficient 0.560449, Coefficient of determination 0.314103, Adjusted Coefficient of determination 0.310388, Standard Error 8.065898 Observations 679. Thus, the Multilinear regression equation with the extracted value of WaterP comes,

$$LST = 32.86 + 0.09 * UrbanP + 0.13 * OpenP + 0.038 * VegP - 0.035 WaterP$$

Where, LST= Land Surface Temperature, 32.86= Intercept, UrbanP= Percentage of Urban, OpenP= Percentage of Open land, VegP= Percentage of Vegetation, WaterP= Percentage of Water

In simple linear regression, relationship between dependent variable and independent variable is

examined. The simple linear regression model use following equation.

$$Y = a + bX + \epsilon$$

Where: y – dependent variable, x – independent variable, a – intercept, b – slope,  $\epsilon$  – residual/error

The simple linear regression for the dependent variable PM2.5, PM10 with independent variable LST is examined for the Summer and Winter seasons. Results are shown below.

For Summer, as shown below in the graph, the Dependent variable is LST, and the independent variable is PM2.5. Regression Statistics derived were Multiple correlation coefficient 0.975516681, Coefficient of determination 0.951632794, Adjusted Coefficient of determination 0.95161155.

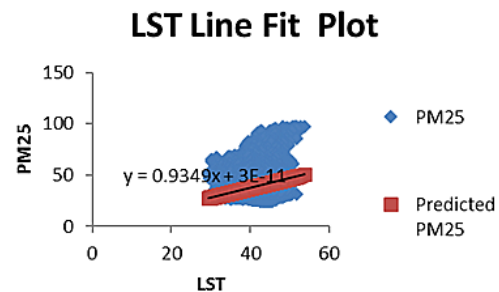


Fig. 10

Now for the Dependent variable as shown below in graph: LST and Independent variable: PM10, Regression Statistics derived were Multiple correlation coefficient 0.97882, Coefficient of determination 0.958088, Adjusted Coefficient of determination 0.958067.

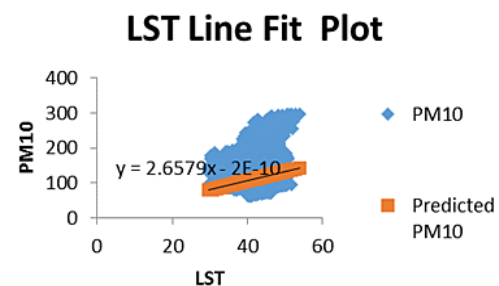


Fig. 11

Regression statistics show a strong positive correlation between PM2.5, PM10 and LST with an R<sup>2</sup> value of 0.95.

For the Winter season, the Dependent variable: LST, Independent variable: PM2.5, and Regression Statistics derived were Multiple correlation coefficient 0.984914728, Coefficient of determination 0.970057021, Adjusted Coefficient of determination 0.970035777.

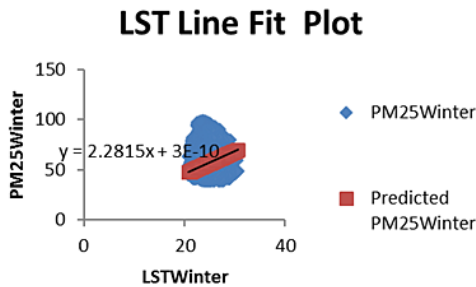


Fig. 12

Now for, Dependent variable: LST, Independent variable: PM10, Regression Statistics derived were Multiple correlation coefficient 0.993962, Coefficient of determination 0.98796, Adjusted Coefficient of determination 0.987938.

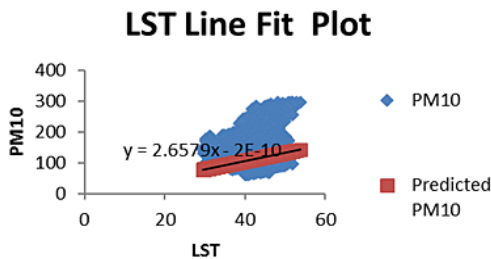


Fig. 13

By analyzing both results, it is seen that in winter correlation between PM2.5 and PM10 with LST is stronger than Summer season. The reason could be a suspended particle-like PM2.5 and PM10 having a higher concentration on the ground in the Winter season than in summer due to low temperature.

After primary data analysis, it is found that Urban Heat Island phenomenon is a problem and needs

to be considered because it is also correlated with Urban Air Quality, and it may affect human health, human comfort, and the environment. Thus, some of these mitigation measures which are being in common practice can be followed as follows:

Since vegetation is negatively correlated with LST, an increment in vegetation area by an act of tree plantation, gardening, or the concept of green building can reduce the intensity of UHI on the city scale.

The surface albedo of material is negatively correlated with LST; thus, the practice of white roofing and material with high solar reflectance can be used as rooftop pavement since they have less solar radiation absorption and higher surface albedo values.

In this study, there are four variables, LST, PM2.5, PM10, and LULC. In order to perform regression analysis, the Multilinear regression method has been used. To predict LST, it is taken as a dependent variable, while LULC classes are taken as independent variables. Regression Statistics derived were Multiple correlation coefficient 0.680257033, Coefficient of determination 0.462749631, Adjusted Coefficient of determination 0.462737156, Standard Error 2.022893242 for observations 209352.

The value of R<sup>2</sup> is 0.46, which is a positive correlation, which means the independent variable explains 46.27% of the variance in the dependent variable.

The multiple linear regression is derived here as,  
 $LST = 34.366 + 0.079 * UrbanP + 0.101 * OpenP + 0.062 * VegP$

Where, LST= Land Surface Temperature, 34.366= Intercept, UrbanP= Percentage of Urban OpenP= Percentage of Open land, VegP= Percentage of Vegetation

The simple linear regression for dependent variable PM2.5, PM10 with independent variable LST is examined for 30m grids. Where, Dependent variable: LST and Independent variable: PM2.5;

Regression Statistics derived were Multiple correlation coefficient 0.013042395, Coefficient of determination 0.000170104, Adjusted Coefficient of determination 0.000165328, Standard Error 9.599812854 for observations 209352.

**LST Line Fit Plot**

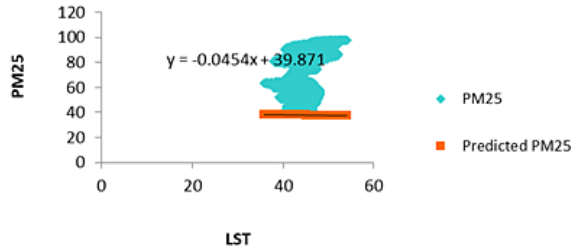


**Fig. 14**

Now for the Dependent variable: LST and Independent variable: PM10; Regression Statistics derived were Multiple correlation coefficient 0.06309568, Coefficient of determination 0.00398107, Adjusted Coefficient of determination 0.00397631, Standard Error 23.0820537, Observations 209352

**LST Line Fit Plot**

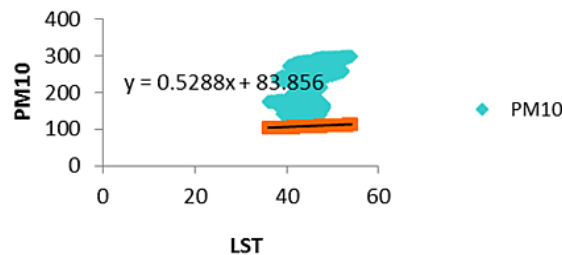


**Fig. 15**

By regression statistics, we have already derived a model equation to predict LST; The multiple linear regression is derived here as,  
 $LST = 34.366 + 0.079 * UrbanP + 0.101 * OpenP + 0.062 * VegP$

Central and West Zone of Ahmedabad is divided into grids of 30m which is the smallest grid size for study and can have an as smallest pixel size of the generated raster of LST, and Land use is

30m (Landsat 8 resolution). Total 209352 polygon rectangular grids are generated with a spatial extent of the central and west zone of Ahmedabad.

As a part of the mitigation strategy, there are two assumptions in which green cover area is increased and proposed with 30% and 40% of the total area of these zones. The predicted LST with proposed Vegetation area cover is as below:

**Table 5**

VegP	UrbanP	OpenP	Existing LST	Predicted LST
30%	50%	20%	42.67	41.66
40%	55%	5%	42.67	41.11



It can be observed that there has been 1 °C temperature decrement in both of these scenarios when green cover is made up 30% and 40%.

Furthermore, PM2.5 and PM10 have been modeled by regression statistics, so the value of Predicted LST can be correlated to Predict PM2.5 and PM10 to get the result as a part of a mitigation strategy in which 30% and 40% Vegetation cover is proposed.

Regression equation for PM10 and PM2.5 has been derived as,

$$PM10 = 0.5288 * LST + 83.856$$

$$PM2.5 = -0.0454 * LST + 39.871$$

If the LST value is replaced with predicted LST, then predicted PM10 and PM2.5 can be derived to estimate the concentration of PM2.5 and PM10.

**Table 6**

Predicted PM2.5	Predicted PM 10	Existing PM2.5	Existing PM10	LST (°C)
37.97	105.88	54.81	156.07	41.66
38.00	105.62	54.81	156.07	41.11

The regression model equation estimates the value of PM 2.5 and PM 10. It is noticeable that the predicted value of PM10 and PM2.5 is 51 mg/m3 and 17 mg/m3 less than existing values.

Central Zone of AMC has a dense typology of building with concrete and metal roof which has low emissivity that absorbs heat, and due to this phenomenon, the temperature rise at the local climatic level can be observed. As a white roof implementation strategy, rooftops with concrete and metal roofs are replaced with white roofs, which affects the local temperature decrement. For this

study, 30% and 40% roofs are converted to white roof for Central Zone of AMC as a mitigation strategy. In Central Zone, 30% and 40% area of the total rooftops are selected so that the raster value of emissivity can be changed with the value of white roof emissivity, which has higher surface reflectivity. It leads to a new LST product because the emissivity of the raster has been modified.

It is noticeable that the area converted 40% under the white roof has a temperature reduction of 1.73°C, while the area converted 40% under the white roof has a temperature reduction of 1.31°C.

**Table 7**

% of White Roof in Area	LST	Predicted PM10	Predicted PM2.5
30%	38.78	104.36	38.10
40%	38.04	103.63	37.47

**Conclusion**

To conclude a study with supportive statistical investigations and results, it can be asserted that Ahmedabad city has been facing both urban heat island phenomena and urban air quality deterioration.

It is observed that seasonal variation affects the formation of Urban Heat Island by accessing decadal data of UHI of the Winter and summer months. From 2008 to 2018 gives an idea that there was an increment in the temperature and air pollution profile.

The land cover maps compared with temperature show that where there is less vegetation, the temperature was high, and the areas with vegetation patches show less temperature than other land use classes.

The correlation analysis was done to model LST, PM2.5, PM10, and LULC. Which shows the positive correlation between land use classes and LST. Moreover, it has been found that there is a strong relationship between PM2.5, PM 10, and LST.

However, it was observed that in the Winter season, the relationship between PM<sub>2.5</sub>, PM<sub>10</sub>, and LST is stronger than in the summer season.

Furthermore, for mitigation strategy, it was considered White Roof mitigation strategy and Green area cover. It is noticeable that both of these mitigation strategies are affecting well to decrease temperature rise in Ahmedabad, It is noticeable that the area converted 40% under the white roof has a temperature reduction of 1.73°C, while the area converted 30% under the white roof has a temperature reduction of 1.31°C. As a part of the green cover increase mitigation strategy, when green cover area is increased and proposed with 30% and 40% of the total zone area there has been 1 °C temperature decrement. Both the strategies also contributes in reduction in the concentration of particulate matter.

The study attempts to establish correlation between the temperature decrease with use of White roof and green cover increment strategy and their

positive impacts on particulate matter concentration reduction of the study area and recommends both mitigation strategies not only to reduce Urban Heat Island Impact but to reduce particulate matter concentrations as well. Use of historical data and remote sensing techniques can be incorporated into urban design and planning for resolution of complex urban climatic issues of air pollution and heat island impacts.

#### Acknowledgement

The author would like to thank, Environment Engineering, Gujarat Technological University, Ahmedabad, India. for their guidance and support to complete this article.

#### Funding

The author(s) received no financial support for the research, authorship, and/or publication of this article.

#### Conflict of Interest

The authors do not have any conflict of interest.

### References

1. Devadas, M. D., & Amirtham, L. R. (2014). Urban Factors and the intensity of Heat Island in the City of Chennai Urban Factors And The Intensity Of Heat Island, (June), 2–6.
2. Estoque, R. C., Murayama, Y., & Myint, S. W. (2017). Science of the Total Environment Effects of landscape composition and pattern on land surface temperature : An urban heat island study in the megacities of Southeast Asia, 577, 349–359.
3. Fortuniak, K. (n.d.). Global environmental change and urban climate in Central European cities.
4. Gill, S., Forest, T. M., & Ennos, R. (2007). Adapting Cities for Climate Change : The Role of the Green Infrastructure, (April 2014). <https://doi.org/10.2148/benv.33.1.115>
5. Golden, J. S., & Golden, J. S. (2010). The Built Environment Induced Urban Heat Island Effect in Rapidly Urbanizing Arid Regions – A Sustainable Urban Engineering Complexity Island Effect in Rapidly Urbanizing Arid Regions – A Sustainable Urban Engineering Complexity, 3430. <https://doi.org/10.1080/15693430412331291698>
6. Heat, U., & Basics, I. (n.d.). Reducing Urban Heat Islands : Compendium of Strategies Urban Heat Island Basics.
7. Imhoff, M. L., Zhang, P., Wolfe, R. E., & Bounoua, L. (2010). Remote Sensing of Environment Remote sensing of the urban heat island effect across biomes in the continental USA, 114, 504–513. <https://doi.org/10.1016/j.rse.2009.10.008>
8. Kotharkar, R., Ramesh, A., Bagade, A., & Asia, S. (2018). Urban Climate Urban Heat Island studies in South Asia : A critical review. *Urban Climate*, (July 2017), 1–16. <https://doi.org/10.1016/j.uclim.2017.12.006>
9. Li, H., Meier, F., Lee, X., Chakraborty, T., & Liu, J. (2018). Interaction between urban heat island and urban pollution island during summer in Berlin *Science of the Total Environment* Interaction between urban heat island and urban pollution island during summer in Berlin, (May). <https://doi.org/10.1016/j.scotot.2018.05.001>

- org/10.1016/j.scitotenv.2018.04.254
10. Li, Z., Tang, B., Wu, H., Ren, H., Yan, G., Wan, Z. Sobrino, J. A. (2013). Remote Sensing of Environment Satellite-derived land surface temperature : Current status and perspectives, 131, 14–37.
  11. Liu, W., You, H., & Dou, J. (2009). Urban-rural humidity and temperature differences in the Beijing area, 201–207. <https://doi.org/10.1007/s00704-008-0024-6>
  12. Taylor, P., Stathopoulou, M., & Cartalis, C. (n.d.). Use of Satellite Remote Sensing in Support of Urban Heat Island Studies Use of Satellite Remote Sensing in Support of Urban Heat Island Studies, (January 2015), 37–41. <https://doi.org/10.1080/17512549.2007.9687275>
  13. UN-Habitat. (2007). World Urbanization Prospects The 2007 Revision Highlights. New York. <https://doi.org/10.2307/2808041>
  14. H. Taha, " Meteorological, air-quality, and emission-equivalence impacts of urban heat island control in California," *Sustainable Cities and Society* 19 (2015) 207–221, 2015.
  15. J Fallman, "Urban Heat Island Versus Air Quality - a Numerical Modelling Study for a European City"(2015)
  16. Roozbeh Arabi, "Mitigating Urban Heat Island Through Green Roofs"(2015). <http://dx.doi.org/10.12944/CWE.10.Special-Issue1.111>